Organic & Biomolecular Chemistry

Accepted Manuscript

This article can be cited before page numbers have been issued, to do this please use: S. Miyamura, M. Araki, Y. Ota, Y. Itoh, S. Yasuda, M. Masuda, T. Taniguchi, Y. Sowa, T. Sakai, T. Suzuki, K. Itami and J. Yamaguchi, *Org. Biomol. Chem.*, 2016, DOI: 10.1039/C6OB01483F.

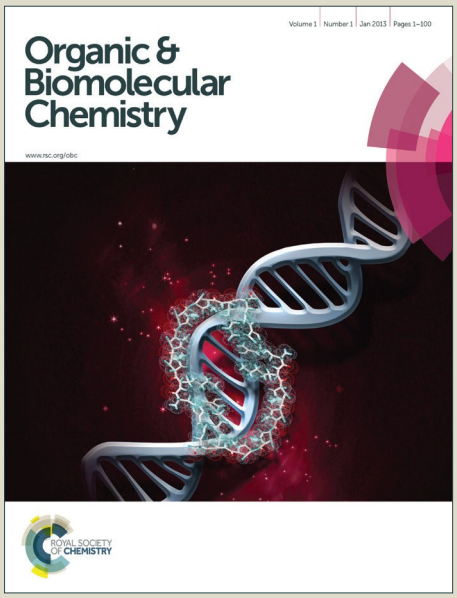

ROYAL SOCIETY OF CHEMISTRY

www.rsc.org/obc

View Article Online
DOI: 10.1039/C6OB01483F

Organic & Biomolecular Chemistry

ARTICLE

C-H Activation Enables Rapid Structure-Activity Relationship Study of Arylcylclopropyl amines for Potent and Selective LSD1 Inhibitors

Shin Miyamura,[1] Misaho Araki,[1] Yosuke Ota,[2] Yukihiro Itoh,[2] Shusuke Yasuda,[2] Mitsuharu Masuda,[2] Tomoyuki Taniguchi,[2] Yoshihiro Sowa,[2] Toshiyuki Sakai,[2,3] Takayoshi Suzuki,*[,2,3] Kenichiro Itami,*[,1, 4] and Junichiro Yamaguchi*[5]

Received 00th January 20xx,
Accepted 00th January 20xx

DOI: 10.1039/x0xx00000x

www.rsc.org/

We describe the structure-activity relationship of various arylcyclopropylamines (ACPAs), which are potent LSD1 inhibitors. More than 45 ACPAs were synthesized rapidly by an unconventional method that we have recently developed, consisting of a C–H borylation and cross-coupling sequence starting from cyclopropylamine. We also generated NCD38 derivatives, which are known as LSD1 selective inhibitors, and discovered a more effective inhibitor compared to the original NCD38.

Introduction

Lysine-specific demethylase 1 (LSD1, KDM1A) is known as an enzyme for the selective demethylation of the fourth methyl/dimethyl lysines on histone H3 (H3K4me1/2). Through flavin adenine dinucleotide (FAD) dependent enzymatic oxidation, LSD1 controls the expression of genes by epigenetics.[1] The structure of LSD1 complexed with CoREST and a histone H3 peptide was first assigned by Yang, Hoelz and coworkers in 2006. [2,3] Ever since the relationship between LSD1 and diseases such as cancer, globin disorder and metabolic syndrome was reported, LSD1 inhibitors have shown promise as an important tool to elucidate the biological function of the enzyme as well as potential epigenetic therapeutic agents including anticancer drugs.[4] Although *trans*-phenylcyclopropylamine (**1a**: PCPA) is known as an LSD1 inhibitor,[5,6] **1a** was showed low inhibitory activity against LSD1 and simultaneously inhibited a FAD dependent oxidation enzymes, mono-amine oxidases (MAOs). Therefore, the development of LSD1-selective inhibitors is in high demand. To enhance the activity and selectivity of **1a** for LSD1, various arylcyclopropylamines (**1**: ACPAs) as LSD1 (selective) inhibitors **2–6** have been synthesized.[7–11] Based on the proposed mechanism of inhibition and the crystal structure of LSD1 with PCPA,[6,12] we developed a cell-active LSD1-selective inhibitor, NCL1 (**7**), which is an amino acid/PCPA (**1a**) hybrid compound.[13,14] Additionally, we developed NCD38 (**8**) as a novel LSD1 selective inhibitor, consisting of a lysine moiety for LSD1 selectivity and a PCPA (**1a**) moiety for LSD1 inhibitory activity.[15]

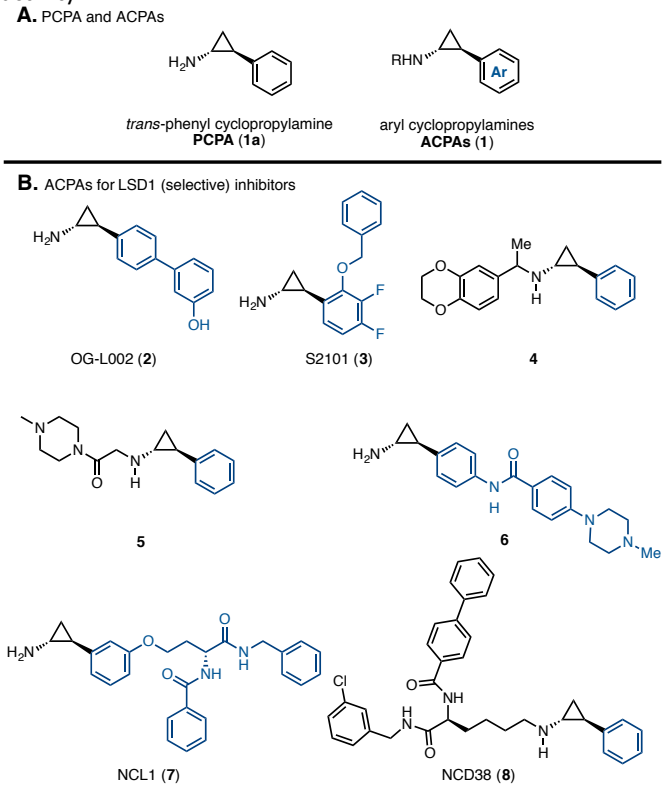

[a] Institute of Transformative Bio-Molecules (WPI-ITbM) and Graduate School of Science, Nagoya University, Chikusa, Nagoya, 464-8602, Japan
[b] Graduate School of Medical Science, Kyoto Prefectural University of Medicine, 1-5 Shimogamo-hangi-Cho, Sakyo-ku, Kyoto, 603-0823, Japan
[c] CREST, Japan Science and Technology Agency (JST), 4-1-8 Honcho Kawaguchi, Saitama 332-0012, Japan
[d] JST, ERATO, Itami Molecular Nanocarbon Project, Nagoya University, Chikusa, Nagoya 464-8602, Japan
[e] Department of Applied Chemistry, Waseda University 3-4-1 Ohkubo, Shinjuku, Tokyo 169-8555, Japan.† Footnotes relating to the title and/or authors should appear here.

Electronic Supplementary Information (ESI) available:. See DOI: 10.1039/x0xx00000x

Figure 1. (A) The structure of PCPA and ACPAs. (B) The structure of ACPAs used as LSD1 (selective) inhibitors.

View Article Online
DOI: 10.1039/C6OB01483F

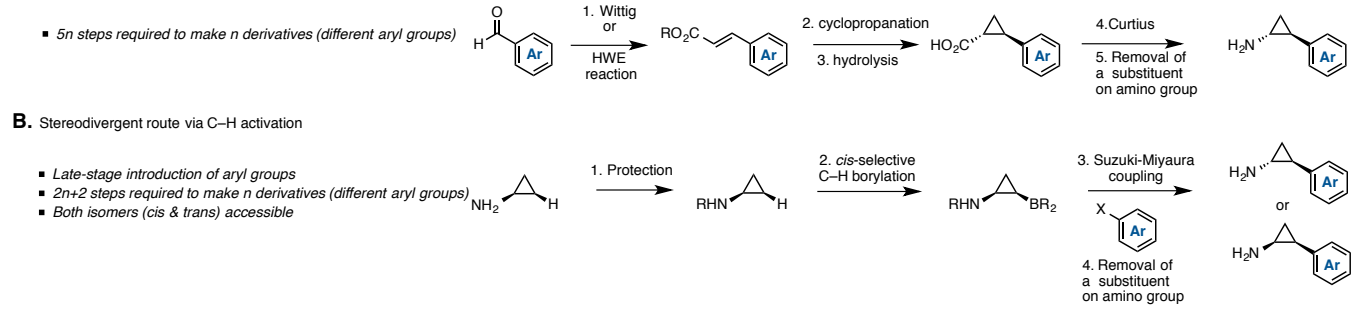

Figure 2. (A) Conventional synthetic route for ACPAs. (B) Rapid and stereodivergent route via C–H activation.

In previous works, some ACPAs showed effective inhibitory activity, however, it was not enough to elucidate a structure-activity relationship (SAR) because of difficulties in accessing structurally diverse analogues. We herein report a rapid synthesis of ACPAs by a C–H activation/Suzuki–Miyaura coupling strategy, which enabled the investigation of its SAR, and the synthesis of NCD38 analogues for structural optimization.

Results and Discussion

Synthesis of ACPAs. A conventional synthetic route for ACPAs (**1**) would necessitate many steps, precisely *5n* steps to make *n* different derivatives (Figure 2A).[16,17] On the other hand, we have developed a rapid and stereodivergent synthesis of ACPAs by C–H activation involving a C–H borylation of cyclopropylamine, followed by a Suzuki–Miyaura cross-coupling reaction (Figure 2B).[18] This synthetic strategy allows for an unconventional bond disconnection and late-stage introduction of different aryl groups on **1** (*2n+2* steps required to make *n* derivatives). Using this method, we synthesized various ACPAs as shown in Table 1.

The synthesis of ACPAs commenced with *N*-cyclopropylpivalamide (**9**), which was reacted with pinacolborane (HBpin) in the presence of catalytic $[Ir(OMe)(cod)]_2$ in cyclohexane at 80 ºC for 18 h to afford the C–H borylation product **10** in 62% yield with virtually complete *cis* selectivity (*cis*/*trans* = >99/1). Then, Pd-catalyzed Suzuki–Miyaura cross-coupling reaction of **10** with various aryl iodides **11** proceeded smoothly under our standard conditions [cat. $PdCl_2(dppf)\cdot CH_2Cl_2$, Ag_2O, Cs_2CO_3, H_2O, 70 °C, under N_2] to give the corresponding coupling products *trans*-**12** and *cis*-**12** (*trans* isomers were the major products).[19] Although the *cis* isomers of **12** can be preferentially synthesized when these reactions are conducted under O_2 atmosphere, O_2 was omitted from the standard reaction conditions because of the lack of stability of many of these *cis* products.[20] After removal of the pivaloyl group on compounds *trans*-**12** under acidic conditions, PCPA (**1a**) and ACPAs **1b–1p** were synthesized.

Synthesis of ACPA Biaryl Derivatives. Next, we synthesized biaryl derivatives of ACPAs **(**BCPAs **16**; Table 2**)** because biaryl compound **1k** showed high inhibitory activity (see, Figure 3 and Table 1). Additionally, since *meta*-fluorophenyl ACPA **1d** also demonstrated inhibitory activity, a hybrid of **1k** and **1d**, *i.e.*, a fluorobiphenyl derivative such as **16h**, was synthesized as well. The synthesis of BCPAs **16a–16ab** was achieved by a simple protection-arylation-deprotection of ACPA **1p** and its defluoro derivative **1q** (Table 2).

Table 1. Synthesis of PCPA (1a) and ACPAs (**1**) by C–H borylation and Suzuki–Miyaura cross coupling reaction.[a]

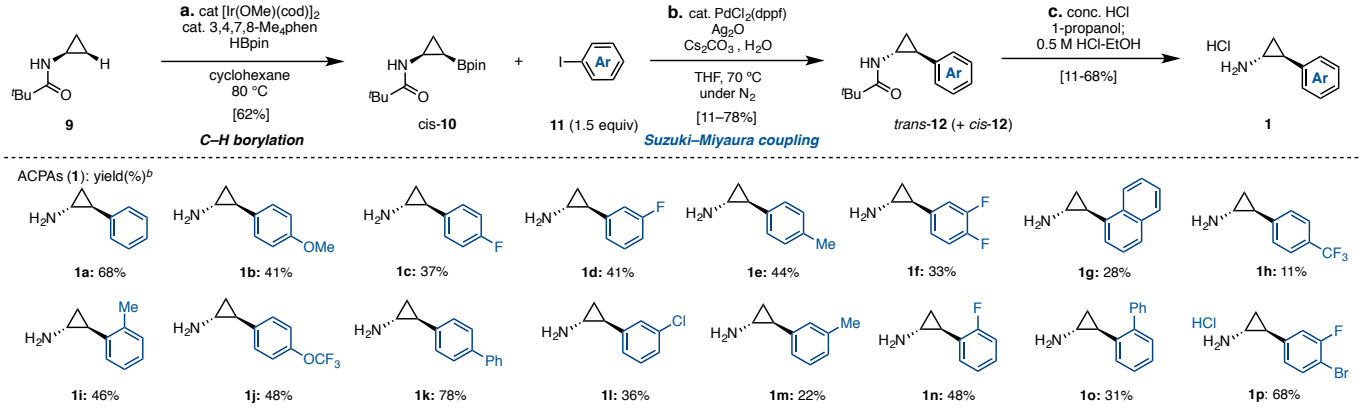

[a]Reagents and conditions: (a) **9** (1.0 equiv), $[Ir(OMe)(cod)]_2$ (0.5 mol%), 3,4,7,8-Me4phen (1.0 mol%), HBpin (1.5 equiv), cyclohexane, 80 °C, 18 h, 62% yield; (b) **10** (1.0 equiv), **11** (1.5 equiv), $PdCl_2(dppf)\cdot CH_2Cl_2$ (8 mol%), Ag_2O (1.5 equiv), Cs_2CO_3 (2.0 equiv), H_2O (2.0 equiv), 70 °C, 6 h, under N_2, 11–78% yield; (c) conc HCl / 1-propanol (1/2), 100 °C, 60 h, 11–68% yield. [b] Yields regard the Suzuki–Miyaura coupling reaction between **10** and **11**. cod = 1,5-cyclooctadiene, HBpin = pinacolborane, 3,4,7,8-Me_4phen = 3,4,7,8-tetramethylphenanthroline. dppf = 1,1'-bis(diphenylphosphino)ferrocene.

View Article Online
DOI: 10.1039/C6OB01487F

Synthesis of NCD38 Derivatives. Finally, NCD38 derivatives were synthesized using ACPAs **1** and BCPAs **16**, whose substituents were selected based on their inhibitory activities for LSD1 (Scheme 3). The original method in the synthesis of NCD38 (**8**) required excess amounts of PCPAs (>10 equiv), in which PCPA carrier moiety **18a** was coupled with PCPA (**1a**).[15]

Table 2. Synthesis of biaryl derivatives of ACPAs (BCPAs 16).[a]

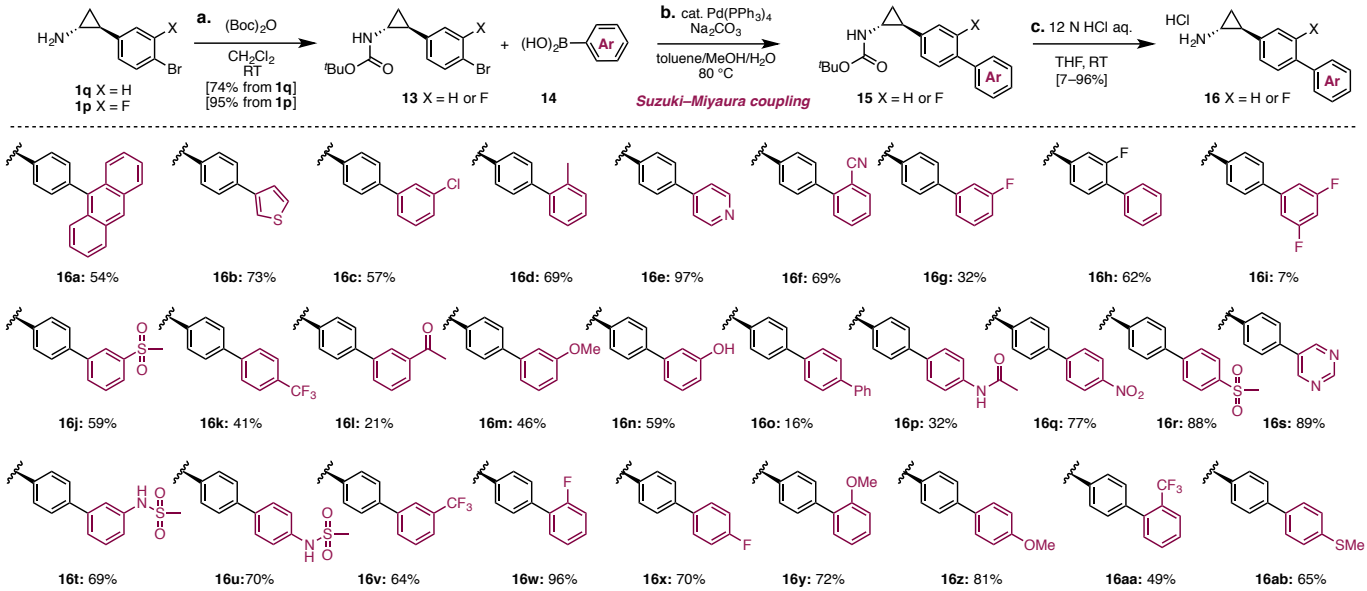

[a]Reagents and conditions: (a) **1q** or **1p** (1.0 equiv), $(Boc)_2O$ (3.0 equiv), CH_2Cl_2, RT, 3 h, 74% yield for **1q**, 95% yield for **1p**; (b) **13** (1.0 equiv), $Pd(PPh_3)_4$ (20 mol%), Na_2CO_3 (2.0 equiv), arylboronic acid **14** (4.0 equiv), water and toluene/MeOH, 80 ºC, 18 h; (c) conc. HCl, THF, RT 7–96% yield over two steps. [b] Yields regard the Suzuki–Miyaura coupling reaction between **13** and **14**.

Table 3. Synthesis of NCD38 derivatives.[a]

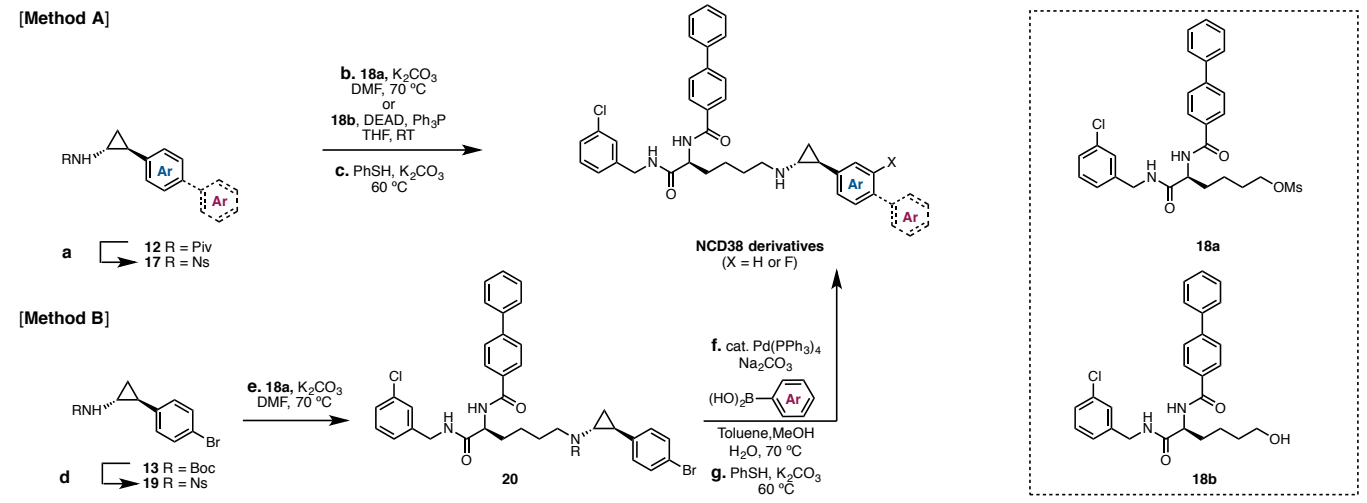

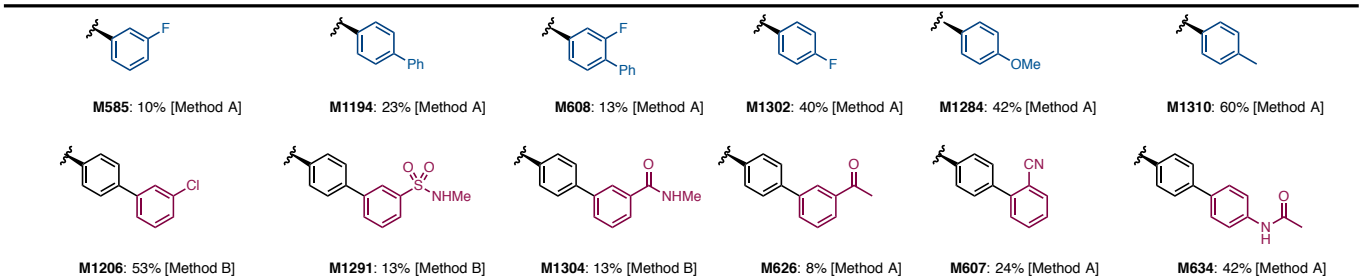

[a]Reagents and conditions: (a) conc. HCl, THF, RT 29–69% yield; then NsCl (1.0 equiv), NEt_3 (2.0 equiv), CH_2Cl_2, RT, 3 h, 23–66% yield. (b) **17** (3.0 equiv), **18a** (1.0 equiv), K_2CO_3 (5.0 equiv), DMF, 70 ºC, 12 h or **17** (3.0 equiv), DEAD (3.0 equiv), PPh_3 (3.0 equiv), THF, RT, 12 h; (c) PhSH (3.0 equiv), K_2CO_3 (4.0 equiv), CH_3CN, 60 ºC, 12 h, 10–42% yield; (d) conc. HCl, THF, RT; (e) **19** (3.0 equiv), **18a** (1.0 equiv), K_2CO_3 (5.0 equiv), DMF, 70 ºC, 12 h, 45–62% yield; (f) **20** (1.0 equiv), $Pd(PPh_3)_4$ (10 mol%), Na_2CO_3 (3.0 equiv), $ArB(OH)_2$, or ArBpin (3.0 equiv), water (0.01 mL) and toluene/MeOH, 70 ºC, 12 h; (g) PhSH (3.0 equiv), K_2CO_3 (4.0 equiv), DMF or CH_3CN, 60 ºC, 12h. 13–53% yield (over two steps). [b] Described yields regard the alkylation reaction of **18a/b** and **17** or **19** and **18a**. DEAD = diethyl azodicarboxylate.

Therefore, we optimized the method by using a nosylation strategy to introduce the carrier moiety **18** more efficiently.[21] The synthesis started from pivalated ACPAs **12**, and exchanging the pivaloyl group (Piv) with nosyl group (Ns) afforded Ns-ACPAs (**17**). Compounds **17** were successfully coupled with PCPA carrier moiety **18a** under basic conditions (K_2CO_3), even when only 3.0 equiv of **17** were used, to give Ns-protected NCD38 derivatives in moderate yields (method A). A Mitsunobu displacement for the coupling of **17** with alcohol **18b** to give the same NCD38 derivatives was also possible. Then, removal of the Ns group with benzenethiol afforded the corresponding NCD38 derivatives in good yields. Alternatively some NCD38 biaryl derivatives were synthesized by a Suzuki–Miyaura cross-coupling of **19** (Ar = 4-bromophenyl) with several arylboronic acids in the presence of a Pd catalyst to give NCD38 derivatives after removal of the Ns group (method B).

LSD1 and MAO Inhibition Activities of ACPAs. Synthesized ACPA analogues **1a–1o** were evaluated for enzyme activity using LSD1 as well as monoamine oxidases, MAO A and MAO B, because LSD1 is structurally similar to MAOs (Figure 3).[22,23] For LSD1, ACPAs **1d**, **1f**, **1h**, **1j**, **1k**, **1l**, and **1n** showed moderate to excellent inhibition compared to PCPA (**1a**) at 10 μM, whereas **1o**, which has a phenyl group at the *ortho*-position of the aryl group did not show LSD1 inhibition. For MAO A and MAO B, all ACPAs **1** displayed moderate to high inhibition, and therefore no LSD1 selectivity was achieved. These results are quite reasonable considering that these ACPAs did not bear a carrier unit such as NCD38 (**8**). Next, the IC_{50} values of PCPA (**1a**) and ACPAs **1c, 1d, 1k, 1h,** and **1l** for LSD1 were also determined (Table 4). PCPA (**1a**) inhibited LSD1 with an IC_{50} value of 80.7 μM, whereas ACPAs **1c, 1d, 1k, 1h,** and **1l** all showed greater LSD1 inhibitory activity (<80 μM). Particularly, the inhibitory activity of ACPA biphenyl derivative **1k** was 34-fold to 59-fold higher than that of **1a** (IC_{50} = 1.37 μM), even though its activity toward MAO A and MAO B was also high (IC_{50} = 0.388 μM for MAO A, IC_{50} = 1.36 μM for MAO B). Encouraged by this finding, we then focused on ACPA biphenyl derivatives **16**, which include fluorophenyl derivatives because the *meta*-fluorophenyl moiety was found to lower the IC_{50} value (**1d** was five-fold more active than **1a,** with an IC_{50} of 14.5 μM).

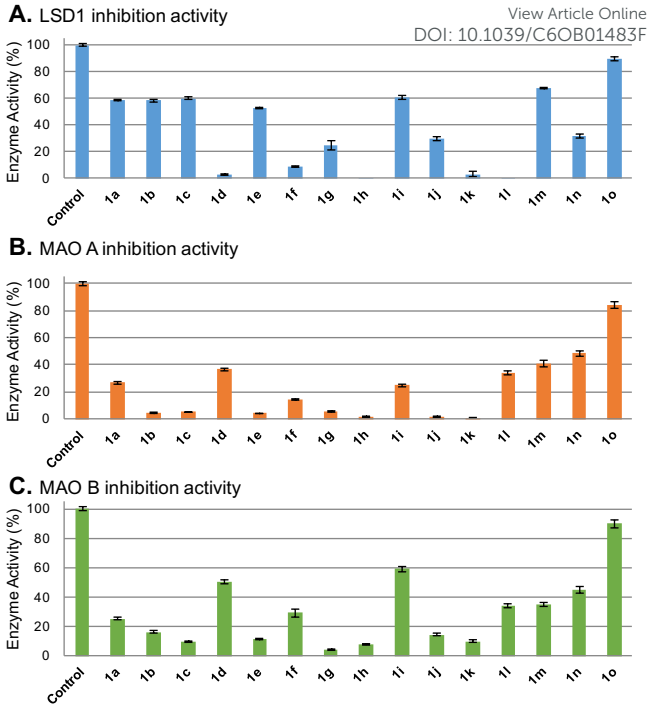

Figure 3. LSD1 and MAO inhibition activity of ACPA derivatives. Compound concentrations for LSD1, MAOA and MAOB are 30 μM, 10 μM and 10 μM, respectively.

Table 4. IC_{50} values of ACPAs 1 against LSD1 and MAOs.

Compound	IC_{50} (μM)[a]		
	LSD1	MAOA	MAOB
1a	80.7±8.0	–	–
1c	79.4±5.0	–	–
1d	14.5±1.1	–	–
1k	1.37±0.01	0.388±0.015	1.36±0.12
1h	11.2±0.5	–	–
1l	12.1±0.3	–	–

[a] These values are the average±SD of at least three experiments.

LSD1 and MAO Inhibition Activities of ACPA Biaryl Derivatives. Synthesized ACPA biaryl derivatives **16** were evaluated for the enzyme activity toward LSD1 and MAOs (Figure 4). ACPA biaryl derivatives **16c**, **16f–16i**, **16k–16r**, **16t–16x**, and **16z** showed higher enzyme activity than for **1k**. Sterically hindered compounds such as **16a** and **16d**, and *N*-heteroaryls such as **16e** and **16s** gave lower enzyme inhibitory activity compared with **1k**. Regarding MAO activity, most compounds **16** gratifyingly showed low enzyme inhibition (thus displaying LSD1 selectivity), with the exception of **16q** for MAO B. We next obtained IC_{50} values for LSD1 for selected compounds that showed high enzyme activity for LSD1 (Table 5).

View Article Online
DOI: 10.1039/C6OB01483E

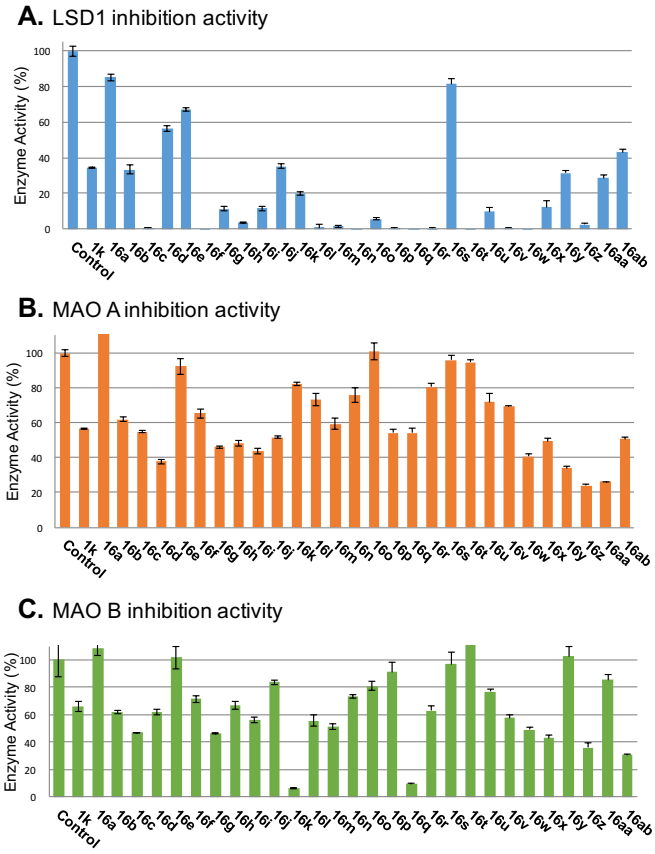

Figure 4. LSD1 and MAO inhibition activity of BCPA derivatives. Compound concentrations for LSD1, MAO A and MAO B are 2 μM, 0.3 μM and 1.0 μM, respectively.

Table 5. IC_{50} values of BCPA derivatives 16 against LSD1.[a]

Compound	LSD1 IC_{50} (μM)[a]
16b	2.40±0.44
16c	2.02±0.45
16d	6.33±0.73
16f	0.388±0.018
16h	1.23±0.10
16l	0.567±0.031
16m	0.173±0.039
16q	0.194±0.008
16r	0.554±0.174

[a] These values are the average±SD of at least three experiments.

LSD1 and MAO Inhibitory Activities of NCD38 Derivatives. We previously identified NCD38, which consists of a PCPA moiety and a lysine structure, as an LSD1 inactivator.14 In our previous study, we optimized the lysine moiety of NCD38 derivatives. However, modification of the PCPA moiety had not been carried out and the SAR remained elusive. Therefore, we attempted to optimize the structure of NCD38 by replacing the phenyl group of PCPA with a substituted phenyl group. Because it was suggested that the lysine structure of NCD38 mimics lysine 4 at histone H3,14 we designed novel LSD1 inhibitors focusing on lysine 4 of histone H3 in the X-ray structure of LSD1 complexed with a propargyllysine H3 peptide (PDB coed 2UXN).11 As shown in Figure 5, we observed some space around the e-amino group of lysine 4. We hypothesized that replacement of the phenyl group of PCPA with a substituted phenyl group could enhance the LSD1-inhibitory activity because the substituted phenyl group could fill that space and interact with amino acid residues such as Met 332, Val 333, Phe 538, Lys 661, Leu659 or Trp695. Based on this hypothesis, we designed new NCD38 derivatives as shown in Table 3.

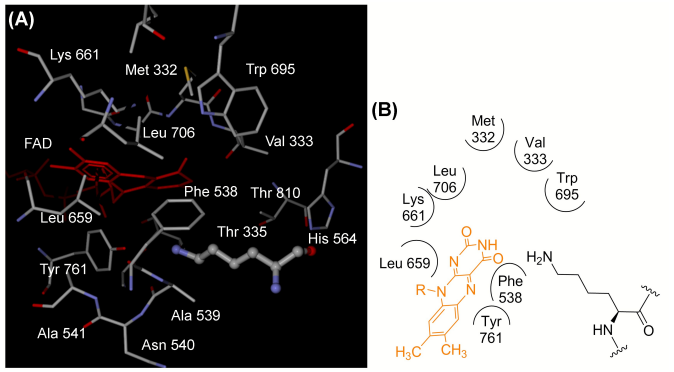

Figure 5. (A) View of the conformation of lysine 4 (ball-and-strick) in histone H3 bound to the LSD1 catalytic site in X-ray structure of LSD1 complexed with a propargylamine-derivatized H3 peptide (PDB code 2UXN). FAD is displayed in the red wire graphic. (B) Schematic diagram of binding of lysine 4 in histone H3 in the LSD1 catalytic site.

The designed NCD38 derivatives were synthesized and evaluated for their inhibitory activity against LSD1 and MAOs (Table 6). Compounds with a small substituent at the *para* or *meta* position of the PCPA (585, 1302, 1284, and 1310) exhibited LSD1-inhibitory activity similar to or slightly weaker than NCD38. Although unsubstituted biphenyl (1194), halogenated biphenyl (608 and 1206), and 2-cyanobiphenyl compounds were inactive, biphenyl compounds bearing a polar functional group at the *meta* or *para* position (1291, 1304, 626, and 634) showed potent LSD1 inhibition. As a result, IC_{50} values in the double-digit nanomolar range were observed with 1304 and 626, which were approximately 6- and 5-fold more potent than NCD38, respectively. In addition, NCD38 derivatives were found to be highly selective inhibitors for LSD1 over MAO A and MAO B.

Table 3. IC_{50} values of NCD38 derivatives against LSD1 and MAOs.[a]

Compound	IC_{50} (μM)		
	LSD1	MAOA	MAOB
NCD38	0.133±0.015	–	–
M585	0.153±0.009	>100	89.0±1.9
M1194	>100	–	–
M608	>100	–	–
M1302	0.346±0.070	>100	45.0±4.4
M1284	0.580±0.052	>100	>100
M1310	0.229±0.022	>100	>100
M1206	>100	–	–
M1291	0.103±0.005	>100	>100
M1304	0.0211±0.0026	>100	>100
M626	0.0275±0.0019	>100	9.28±0.92
M607	>100	–	–
M634	0.183±0.015	49.4±3.3	>100

[a] These values are the average±SD of at least three experiments.

Effect of NCD38 Derivatives on Cancer Cells. As shown in Table 6, eight NCD38 derivatives (M585, M1302, M1284, M1310, M1291, M1304, M626 and M634) showed potent and selective LSD1-inhibitory activity with IC_{50} values lower than 1 μM. These eight derivatives were tested for their growth inhibitory activity against cancer cells. For this study, we chose lung cancer A549 cells because LSD1 is overexpressed in this cell line and the siRNA-mediated LSD1 knockdown induces the growth inhibition of A549 cells.[24,25] As shown in Figure 6, M585, M626 and M634 had little influence on the A549 cell growth at 10 μM, and M1291 slightly inhibited the A549 cell growth. The cell growth inhibitory activities of M1302, M1284, and M1304 were moderate (60–70% inhibition at 10 μM). M1310 as well as NCD38 completely inhibited the growth of A549 cells at 10 μM. Then, we determined the GI_{50} values of compounds whose inhibitory activity was more than 50% at 10 μM. As a result, the GI_{50} value of M1310 was superior to that of NCD38, M1302, M1284 and M1304 (Table 7). Thus, M1310 was the most potent LSD1 inhibitor identified in the A549 cell growth inhibitory assays.

Table 4. GI_{50} values of NCD38 and its derivatives against lung cancer A549 cells.

Compound	GI_{50} (μM)[a]
NCD38	8.60 ± 0.20
M1302	9.19 ± 0.32
M1284	9.12 ± 0.17
M1310	6.17 ± 0.017
M1304	9.32 ± 0.13

[a] Values are means of at least three experiments.

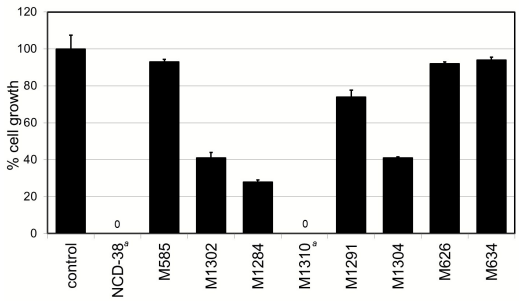

Figure 6. Cell growth inhibition with treatment of lung cancer A549 cells with 10 μM of NCD38 or its derivatives. Error bars represent the mean ± standard deviation (SD) of at least three samples. [a] these compounds completely inhibited the cancer cell growth at 10 μM.

We also investigated the effects of M1310 on cell cycle progression of A549 cells by FACS analysis. M1310 at 2 μM or more for 24 h significantly increased the population of G1 phase with a decrease of the S phase (Figure 7A), indicating that M1310 arrests the cell cycle at the G1 phase. Furthermore, 6 and 8 μM of M1310 increased the sub-G1 phase in a time-dependent manner (Figure 7B).

To investigate whether M1310 inhibits LSD1 in cells, we performed a cellular assay with Western blot analysis. Since LSD1 catalyzes the demethylation of H3K4me2 and H3K4me1, we evaluated the levels of methylation of H3K4 in A549 cells treated with M1310 (Figure 8). As a result, the treatment with M1310 for 24 h induced the accumulation of H3K4me3, H3K4me2, and H3K4me1 in a dose-dependent manner. An increase of the trimethylation of H3K4 is reasonable because LSD1 has been reported to regulate the levels of H3K4me2 and H3K4me1 directly, and then subsequently regulate the level of H3K4me3, at the promoters of some genes.[26,27] Therefore, these results demonstrate that M1310 inhibits LSD1 in A549 cells.

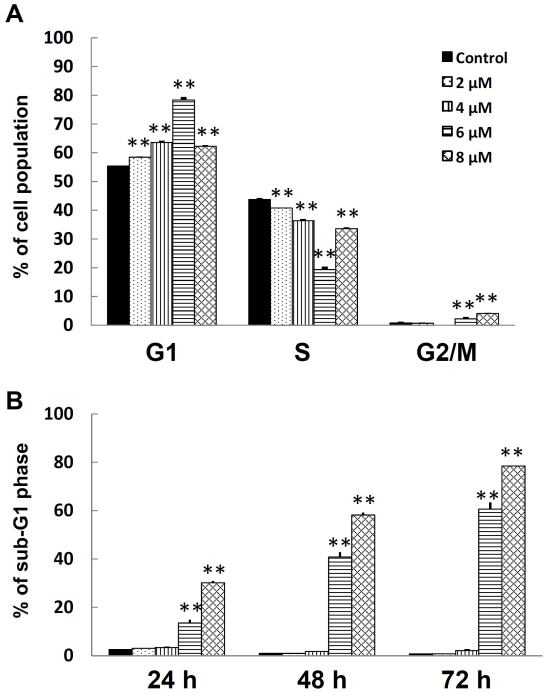

Figure 7. Induction of G1 phase arrest and apoptosis in lung cancer A549 cells by M1310. A549 cells were treated with the indicated concentrations of M1310 for 24, 48 or 72 h. The population of each cell cycle at 24 h (A) and apoptosis at 24, 48 or 72 h (B) was determined using FACS analysis. Data are shown as the means ± SD (n = 3). **: P<0.01 vs. control.

View Article Online
DOI: 10.1039/C6OB01483F

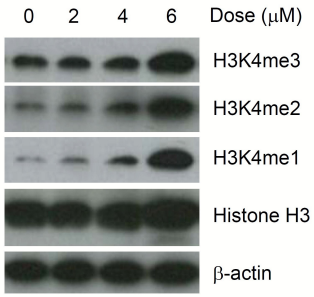

Figure 8. Accumulation of methylated histone H3K4 in lung cancer A549 cells by M1310. Western blotting for tri-methylated histone H3K4 (H3K4me3), di-methylated histone H3K4 (H3K4me2), mono-methylated histone H3K4 (H3K4me1), and total histone H3 was performed with lysates of the cells treated for 24 h with the indicated concentrations of M1310. β-actin is shown as a loading control.

Effect of M1310 on in vivo tumor progression. Finally, we evaluated the effects of M1310 in the A549 xenograft model. A549 cells were inoculated subcutaneously in nude mice. M1310 was intravenously injected (1 mg/kg/day, thrice a week) for 6 weeks. As shown in Figure 9A, tumor growth was suppressed in M1310 group compared to the vehicle group. The toxicity of M1310 was also assessed by measuring the body weight of the mice. M1310 administration did not show any difference in the body weight gain compared to the vehicle during treatment (Figure 9B).

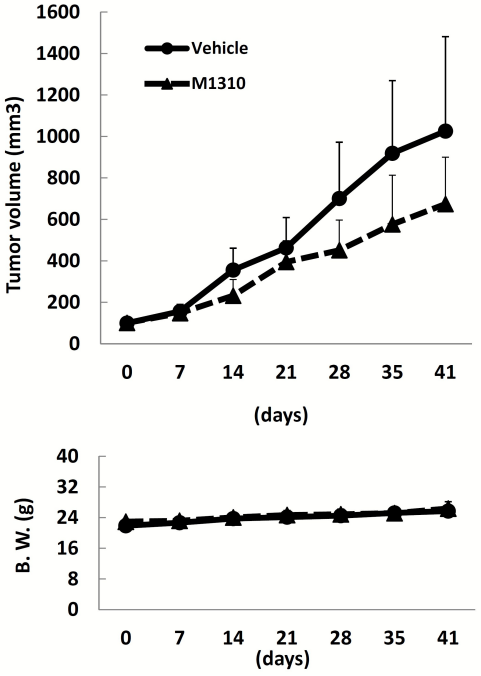

Figure 9. Effects of M1310 on tumor volume and body weight in the lung cancer A549 lung cancer xenograft model. A total of 4.1 x 106 A549 lung cancer cells per mouse were subcutaneously inoculated into nude mice. M1310 (1 mg/kg/day thrice a week; triangle) or vehicle (circle) was intravenously injected for 6 weeks. Tumor volume (A) and body weight (B) of the mice were measured once a week. Data are shown as the means ± SD (n = 6).

Conclusions

In conclusion, we prepared more than 45 ACPAs possessing various aryl groups at the C2-position of the cyclopropylamine, by a C–H activation/Suzuki–Miyaura coupling strategy. The SAR and optimization study of the ACPAs identified BCPAs such as **16n** and **16q** as potent LSD1 inhibitors. We also prepared twelve NCD38 derivatives with various ACPAs, and identified potent LSD1-selective inhibitors such as M1310. M1310 strongly inhibited the growth of lung cancer A549 cells by a G_0/G_1 arrest of the cell cycle and apoptosis induction. M1310 induced a dose-dependent increase of methylated Lys4 of histone H3 in A549 cells, suggesting its intracellular LSD1-inhibitory activity. Furthermore, M1310 exhibited in vivo anticancer activities in the A549 xenograft model. We believe that M1310 will be a useful tool for probing the biology of LSD1, and is also a candidate agent, or at least a lead compound, for cancer treatment. We also believe that the C–H activation/Suzuki–Miyaura coupling methodology is of value in future studies for the development of more potent and selective LSD1 inhibitors as well as other biologically active compounds containing an ACPA structure.[28] This synthetic approach will find use in many areas to rapidly identify novel and highly potent/selective bio-functional molecules.

Materials and methods

Chemistry. Unless otherwise noted, all reactants or reagents including dry solvents were obtained from commercial suppliers and used as received. $[Ir(OMe)(cod)]_2$ was obtained from Sigma-Aldrich. 3,4,7,8-Me_4phen and HBpin were obtained from TCI Chemical. $PdCl_2(dppf)\cdot CH_2Cl_2$, Ag_2O and Cs_2CO_3 were obtained from Wako Chemicals. Unless otherwise noted, all reactions were performed with dry solvents under an atmosphere of nitrogen in dried glassware using standard vacuum-line techniques. All Suzuki–Miyaura coupling reactions were performed in 20-mL glass vessel tubes equipped with J. Young® O-ring tap and heated in a heating block. All work-up and purification procedures were carried out with reagent-grade solvents in air. Analytical thin-layer chromatography (TLC) was performed using E. Merck silica gel 60 F254 precoated plates (0.25 mm). The developed chromatogram was analyzed by UV lamp (254 nm) or phosphomolybdic acid/sulfuric acid solution. Flash column chromatography was performed with E. Merck silica gel 60 (230–400 mesh). Medium pressure liquid chromatography (MPLC) was performed using a Yamazen W-prep 2XY. Preparative thin-layer chromatography (PTLC) was performed using Wakogel B5-F silica coated plates (0.75 mm) prepared in our laboratory. The high-resolution mass spectra were conducted on a Thermo Fisher Scientific Exactive (ESI) and a JMS-T100TD instrument (DART). Nuclear magnetic resonance (NMR) spectra were recorded on a JEOL JNM-ECA-600 spectrometer (^{1}H 600 MHz, ^{13}C 150 MHz), a JEOL JNM-ECA-500 spectrometer (^{1}H 500 MHz, ^{13}C 125 MHz), a Bruker AVANCE III HD (^{1}H 500 MHz, ^{13}C 125 MHz) and a Bruker AVANCE III NanoBay (^{1}H 400 MHz, ^{13}C 100 MHz). Chemical shifts for ^{1}H NMR are expressed in parts per million (ppm) relative to tetramethylsilane (δ 0.00 ppm). Chemical shifts for ^{13}C NMR are expressed in ppm relative to $CDCl_3$ (δ 77.0 ppm) or DMSO-d_6 (δ 39.5 ppm). Data are reported as follows: chemical shift, multiplicity (s = singlet, d =

View Article Online
DOI: 10.1039/C6OB01487F

doublet, dd = doublet of doublets, t = triplet, dt = doublet of triplets, td = triplet of doublets, q = quartet, m = multiplet, brs = broad singlet), coupling constant (Hz), and integration. Infrared spectra were recorded on a JASCO FT/IR-6100 spectrometer. Melting points were measured on a MPA100 OptiMelt automated melting point system. Purity of all test compounds was >95% determined by Waters Acquity H Class, Acquity UPLC BEH C18 1.7 mm 2.1 x 30 mm column, gradient: A/B = 95/5 to 0/100 over 1.5 min, 1 mL/min, solvent A: 0.05% TFA in H_2O, solvent B: 0.05% TFA in acetonitrile.

General Procedure for Deprotection of Pivalamide 12. To a mixture of *trans*-**12** in 1-PrOH (2 mL) was added conc. HCl (1 mL). The mixture was heated at 100 °C for 60 h in a test tube in oil bath. After cooling to room temperature, the reaction mixture was poured into water (5 mL). The aqueous phase was washed with ethyl acetate (5 mL x 2) and basified with 5N NaOH. The basic aqueous phase was extracted with ethyl acetate (5 mL x 2). The combined organic layers were washed with water (10 mL x 1) and brine (5 mL x 2), dried over Na_2SO_4, and concentrated *in vacuo* to afford arylcyclopropylamine **1**. The obtained arylcyclopropylamine **1** was dissolved into 0.5 M HCl-EtOH (1 mL). Then, the volatiles were evaporated *in vacuo*. The resultant residue was washed with ethyl acetate to afford HCl salt of **1**.

General Procedure for Preparation of Biphenyl Derivatives. To a solution of **1q** (299 mg, 1.41 mmol, 1.0 equiv) in CH_2Cl_2 (7.1 mL) was slowly added $(Boc)_2O$ (0.98 mL, 4.23 mmol, 3.0 equiv) at 0 °C. The reaction mixture was stirred for 3 h at room temperature. The volatiles were evaporated *in vacuo*. The resultant residue was purified by silica gel column chromatography (hexane/ethyl acetate = 5:1 to 3:1) to give 327 mg of **13** as a white solid in a 74% yield. Then, a 20-mL glass vessel equipped with J. Young® O-ring tap containing a magnetic stirring bar was flame-dried under vacuum and filled with nitrogen after cooling to room temperature. A mixture of the protected amine **13** (60 mg, 0.19 mmol, 1.0 equiv), $Pd(PPh_3)_4$ (43.9 mg, 0.04 mmol, 20 mol%), Na_2CO_3 (40.3 mg, 0.38 mmol, 2.0 equiv), and arylboronic acid **14** (0.76 mmol, 4.0 equiv) were added to this tube and dissolved into water (0.01 mL) and toluene/MeOH (0.54 mL/0.12 mL). The mixture was heated at 80 °C for 18 h in oil bath under N_2. After cooling to room temperature, the mixture was diluted with ethyl acetate. The insolubles were filtered off through Celite® and the filtrate was concentrated *in vacuo*. The resultant residue was purified by flash column chromatography (hexane/ethyl acetate = 3:1 to 2:1) to afford the coupling product **15**. The obtained coupling product was dissolved into THF (1.0 mL) and added 12 N HCl aq. (1.0 mL). The reaction mixture was stirred for 12 h at room temperature. The volatiles were evaporated *in vacuo* and washed with ethyl acetate to afford HCl salt of **16**.

General procedure for Synthesis of NCD derivatives, M1302, M1284, and M1310. To a solution of **18b**[14] (1.0 equiv), the nosylate **17** (1.1 equiv) and PPh_3 (3.0 equiv) in THF (0.03 M) was slowly added 40% DEAD in toluene (3.0 equiv). The reaction mixture was stirred at room temperature overnight. The volatiles were evaporated *in vacuo*. The resultant residue was purified by MPLC (hexane/ethyl acetate = 1:1 to 0:1) to give the crude product. The ^1H NMR spectrum of this compound was consistent with the desired product though some impurities were included. To a suspension of the obtained crude nosylate (1.0 equiv) and K_2CO_3 (4.0 equiv) in CH_3CN (0.04 M) was added PhSH (3 equiv.). The reaction mixture was stirred overnight at 60 ºC. After cooling to room temperature, the reaction mixture was diluted with water and extracted with ethyl acetate. The combined organic layers were washed with brine, dried over Na_2SO_4, and concentrated *in vacuo*. The resultant residue was purified by NH-MPLC (hexane/ethyl acetate = 1:1 to 0:1) to give the desired product.

LSD1 Inhibition Assay (*In vitro* enzyme assay). LSD1 activity assays were performed using an LSD1 fluorescent assay kit (Enzo life science, BML-AK544-0001). Inhibitor candidates were added to an enzyme solution of LSD1 (0.5 μg/well) and HRP on ice, and then reactions were initiated by addition of a substrate solution of H3K4me2 peptide (4.6 μg/well) and CeLLestial™ Red into all but the blank wells. After incubation (room temperature; 30 min), the fluorescence of the wells was measured on a 2030 ARVO™ X3 multilabel reader (PerkinElmer; excitation: 540 nm; detection: 590 nm) and the % of inhibition was calculated from the fluorescence readings of inhibited wells relative to those of control wells. The concentration of test compounds that resulted in 50% inhibition was determined by plotting log [Inh] against the logit function of the % inhibition. IC_{50} values were determined by regression analysis of the concentration/inhibition data.

MAO Inhibition Assays (*In vitro* enzyme assays). The MAO activity assays were carried out according to the supplier's protocol using a MAO-Glo™ assay system (Promega, V1401). MAOA (18 unit/mL) or MAOB (6 unit/mL) (Sigma-Aldrich; 25 μL/well), 160 μM (for MAOA) or 16 μM (for MAOB) (4*S*)-4, 5-dihydro-2-(6-hydroxybenzothiazolyl)-4-thiazolecarboxylic acid (12.5 μL/well), a MAO substrate, and various concentrations of inhibitors (12.5 μL/well) were incubated at room temperature. Reactions were stopped after 60 min by adding reconstituted Luciferin Detection Reagent (50 μL/well). Then, 20 minutes after addition of this reagent, the chemiluminescence of the wells was measured with a 2030 ARVO™ X3 multilabel reader (PerkinElmer). For the data processing, the same procedure as for LSD1 inhibition activity was used.

Cell viability assay. Lung cancer A549 cells were plated in 96-well plates at the initial density of 1 x 10^3 cells/well (50 mL/well) and incubated at 37°C. After 24 h, cells were exposed to test compounds by adding solutions (50 mL/well) of the compounds at various concentrations in medium at 37 °C under 5% CO_2 in air for 72 h. The mixtures were then treated with 10 mL of AlamarBlue® (AbD Serotec, #BUF012A), and incubation was continued at 37 °C for 3 h. The fluorescence in each well was measured with an ARVO™ X3 microplate reader (excitation at 540 nm, emission, at 590 nm). The percentage cell growth was calculated from the fluorescence readings.

Analysis of cell cycle population and detection of apoptosis. Cells were incubated with the indicated concentrations of M1310. After washing with PBS, the cells were treated with Triton X-100, and the nuclei were stained with propidium iodide. The DNA content was measured using FACSCalibur

(Becton Dickinson, Franklin Lakes, NJ, USA). The ModFit software (Verity Software House, Topsham, ME, USA) and CellQuest (Becton Dickinson) software were used to analyze the data.

Western Blot Analysis. Cells were incubated with the indicated concentrations of M1310 for 24 h. After washing with PBS, the cells were lysed in lysis buffer containing 50 mM Tris-HCl [pH8.0], 150 mM NaCl, 1% NP-40, 0.5% deoxycholic acid, 0.1% SDS, 1 mM EDTA, 1 mM DTT, 0.5 mM PMSF, 2 mg/mL aprotinin, 2 mg/mL leupeptin, and phosphatase inhibitor cocktail (1/100 v/v, 07575-51, Nacalai Tesque, Kyoto, Japan). The lysate was sonicated and centrifuged, and the supernatant was subjected to SDS-PAGE. Rabbit monoclonal anti-histone H3K4me3 (#9751), histone H3K4me2 (#9725), histone H3K4me1 (#5326), histone H3 (#4499, Cell Signaling Technology, Danvers, MA, USA), and mouse monoclonal anti-β-actin (A5441, Sigma, St. Louis, MO, USA) antibodies were used as the primary antibodies. The blots were incubated with the appropriate HRP-conjugated secondary antibody (GE Healthcare, Piscataway, NJ, USA), and signals were detected with Chemi-Lumi One L (Nacalai Tesque) or Immobilon Western (Millipore, Bedford, MA, USA).

Anti-tumor study in xenograft model. Five week-old male BALB/c nu/nu mice were obtained from Shimizu Laboratory Supplies Co., Ltd. (Kyoto, Japan). A total of 4.1 x 10^6 A549 cells with Matrigel Basement Membrane Matrix (Corning, Corning, NY, USA) was subcutaneously inoculated into the left flank of the mice. When the mean tumor volume reached 100 mm^3, the mice were randomized into two groups, and M1310 solved in PBS containing 15% NIKKOL HCO-60 (PHARM) or vehicle was intravenously injected thrice a week for 6 weeks. NIKKOL HCO-60 (PHARM) was provided from Nikko Chemicals Co., Ltd. (Tokyo, Japan). Tumor volume was measured once a week with a caliper and calculated by the following formula: 1/2 x (length x width^2). Body weight was also measured once a week. All experiments and procedures were performed in accordance with the Institutional Care Use Committee guidelines.

Statistical analysis. Statistical analysis was performed using Dunnett's test. $P<0.05$ was considered significant.

Acknowledgements

We thank Mie Morita for technical support. This work was supported by KAKENHI (16H01140 and 16H04148 to J.Y.) from MEXT, and JST CREST program (T.S.). ITbM is supported by the World Premier Interntional Research Center (WPI) Initiative, Japan.

Notes and references

1 Y. Shi, F. Lan, C. Matson, P. Mulligan, J. R. Whetstine, P. A. Cole, R. A. Casero, and Y. Shi, *Cell,* 2004, **119**, 941–953.
2 M. Yang, C. B. Gocke, X. Luo, D. Borek, D. R. Tomchick, M. Machius, Z. Otwinowski, and H. Yu, *Mol. Cell,* 2006, **23**, 377–387.
3 P. Stavropoulos, G. Blobel, and A. Hoelz, *Nat. Struct. Mol. Biol.,* 2006, **13**, 626–632.
4 X. Wang, B. Huang, T. Suzuki, X. Liu, and P. Zhan, *Epigenomics*, 2015, **7**, 1379–1396.
5 D. M. Schmidt, and D. G.McCafferty, *Biochemistry,* 2007, **46**, 4408–4416.
6 M. Yang, J. C. Culhane, L. M. Szewczuk, P. Jalili, H. L. Ball, M. Machius, P. A. Cole, and H. Yu, *Biochemistry,* 2007, **46**, 8058–8065.
7 S. Mimasu, N. Umezawa, S. Sato, T. Higuchi, T. Umehara, and S. Yokoyama, *Biochemistry,* 2010, **49**, 6494–6503.
8 Y. Liang, D. Quenelle, J. L. Vogel, C. Mascaro, M. A. Ortega, and T. M. A. Kristie, *mBio.,* 2013, **4**, e00558.
9 M. A. Ortega, L. J. Castro-Palomino, and M. C. T. Fyfe, Patent application WO 2011035941, 2011.
10 R. Neelamegam, E. L. Ricq, M. Malvaez, D. Patnaik, S. Norton, S. M. Carlin, I. T. Hill, M. A. Wood, S. J. Haggarty, and J. Hooker, *ACS Chem. Neurosci*., 2012, **3**, 120–128.
11 M. Yang, J. C. Culhane, L. M. Szewczuk, C. B. Gocke, C. A. Brautigam, D. R. Tomchick, M. Machius, P. A. Cole, and H. Yu, *Nat. Struct. Mol. Biol.,* 2007, **14**, 535–539.
12 P. Vianello, O. A. Botrugno, A. Cappa, R. Dal Zuffo, P. Dessanti, A. Mai, B. Marrocco, A. Mattevi, G. Meroni, S. Minucci, G. Stazi, F. Thaler, P. Trifiró, S. Valente, M. Villa, M. Varasi, and C. Mercurio, *J. Med. Chem.,* 2016, **59**, 1501.
13 R. Ueda, T. Suzuki, K. Mino, H. Tsumoto, H. Nakagawa, M. Hasegawa, R. Sasaki, T. Mizukami, and N. Miyata, *J. Am. Chem. Soc.,* 2009, **131**, 17536–17537.
14 D. Ogasawara, T. Suzuki, K. Mino, R. Ueda, M. N. Khan, T. Matsubara, K. Koseki, M. Hasegawa, R. Sasaki, H. Nakagawa, T. Mizukami, and N. Miyata, *Bioorg. Med. Chem.,* 2011, **19**, 3702–3708.
15 D. Ogasawara, Y. Itoh, H. Tsumoto, T. Kakizawa, K. Mino, K. Fukuhara, H. Nakagawa, M. Hasegawa, R. Sasaki, T. Mizukami, N. Miyata, and T. Suzuki, *Angew. Chem. Int. Ed.,* 2013, **52**, 8620–8624.
16 D. M. Gooden, D. M. Schmidt, J. A. Pollock, A. M. Kabadi, and D. G. McCafferty, *Bioorg. Med. Chem. Lett.,* 2008, **18**, 3047–3051.
17 H. Benelkebir, C. Hodgkinson, P. J. Duriez, A. L. Hayden, R. A. Bulleid, S. J. Crabb, G. Packham, and A. Ganesan, *Bioorg. Med. Chem.,* 2011, **19**, 3709–3716.
18 S. Miyamura, M. Araki, T. Suzuki, J. Yamaguchi, and K. Itami, *Angew. Chem. Int. Ed*., 2015, **54**, 846–851.
19 Although the precise mechanism remains unclear, epimerization occurred at the nitrogen-bound carbon atom under N_2 atmosphere. See details in ref. 17.
20 During removal of pivaloyl group and thereafter, the epimerization also occurred to afford *trans*-ACPA derivatives.
21 T. Kan, and Fukuyama, *Chem. Commun.,* 2004, 353–359.
22 D. M. Schmidt, and D. G. McCafferty, *Biochemistry,* 2007, **46**, 4408–4416.
23 G. W. Humprey, Y. Wang, V. R. Russanova, T. Hirai, J. Qin, Y. Nakatani, and B. H. Howard, *J. Biol. Chem*., 2001, **276**, 6817–6824.
24 T. Lv, D. Yuan, X.Miao, Y. Lv, P. Zhan, X. Shen, Y. Song, *PLoS ONE* 2012, **7**, e35065.
25 S. Hayami, J. D. Kelly, H. S. Cho, M. Yoshimatsu, M. Unoki, T. Tsunoda, H. I. Field, D. E. Neal, H. Yamaue, B. A. Ponder, Y. Nakamura, and Hamamoto, R. *Int. J. Cancer,* 2011, **128**, 574–586.
26 C. T. Foster, O. M. Dovey, L. Lezina, J. L. Luo, T. W. Gant, N. Barlev, A. Bradley, and S. M. Cowley, *Mol. Cell Biol.,* 2010, **30**, 4851–4863.
27 A. Adamo, B. Sesé, S. Boue, J. Castaño, I. Paramonov, and M. J. Barrero, *Nat. Cell Biol.,* 2011, **13**, 652–659.
28 M. N. A. Khan, T. Suzuki, and N. Miyata, *Med. Res. Rev.,* 2013, **33**, 873–910.